Thermochimica Acta 503–504 (2010) 46–54

Contents lists available at ScienceDirect

Thermochimica Acta

journal homepage: www.elsevier.com/locate/tca

Thermodynamic investigation of lime-enhanced molybdenite reduction using methane-containing gases

Samad Ghasemi Najafabadi*, Mohammad Hasan Abbasi, Ali Saidi

Materials Engineering Department, Isfahan University of Technology, Isfahan 84156-83111, Iran

ARTICLE INFO

Article history:
Received 1 December 2009
Received in revised form 28 February 2010
Accepted 5 March 2010
Available online 16 March 2010

Keywords:
Molybdenite
Lime
Methane
Reduction
Stability diagrams
Carbon deposition

ABSTRACT

Lime-enhanced molybdenite reduction (LEMR) with methane-containing gases has been thermodynamically studied. The reaction proceeds through the direct oxidation of MoS_2 by CaO to form intermediate molybdenum oxidized species, MoO_2 and $CaMoO_4$. The thermodynamics of Mo–O–C–H and Mo–Ca–O–C–H systems has been investigated instead of Mo–Ca–S–O–C–H system, as the sulfur is captured by calcium and forms a neutral compound (i.e. calcium sulfide). The role of reducing agent is the reduction of these oxidized species. Reduction of oxidized species by methane will yield Mo, Mo_2C or MoC. The thermodynamic investigation resulted in construction of stability diagrams of molybdenum compounds. These diagrams were constructed for CH_4–H_2, CH_4–H_2–Ar and CH_4–CO_2–H_2O gas mixtures. In addition to stability regions of Mo, Mo_2C and MoC, the carbon deposition area was also identified. The results showed that by using appropriate gas composition and temperature, different molybdenum-containing phases would be stable thermodynamically while soot formation can be avoided.

1. Introduction

Molybdenite concentrate is the major starting material for pyrometallurgical processing of molybdenum. The extraction of molybdenum from this mineral is technically difficult and economically important. Almost all molybdenite concentrates are first subjected to roasting to yield technical grade molybdic oxide. This compound is the basic raw material for production of molybdenum. In addition to technical difficulties during roasting step (such as low recovery of molybdenum) there is environment pollution with SO_2 [1]. Due to these problems, in the last three decades numerous alternative approaches have been proposed for the production of molybdenum from MoS_2 concentrates [1]. So far, none of these methods has gained any commercial approval.

Another new concept for the winning of metals from their sulfides is their direct reduction in the presence of lime. Many researchers have investigated the thermodynamic and kinetic aspects of molybdenite processing by such an approach. Mankhand et al. [2,3] evaluated the lime-enhanced hydrogen reduction of molybdenite. The required partial pressure of hydrogen for the molybdenum metal formation at different temperatures has been calculated. Thermodynamic and kinetic investigation of carbothermic LEMR was carried out by Padilla et al. [4] where the stability areas of different molybdenum-containing phases have been identified and presented by stability diagrams. Prasad et al. [5] investigated the thermodynamics of LEMR by carbon monoxide. To understand the direct synthesis of Mo_2C by the lime–molybdenite–carbon monoxide reaction, lime-enhancement diagrams were constructed. In these diagrams, the required partial pressure range of carbon monoxide for Mo_2C formation has been demonstrated. The kinetics of carbon monoxide reduction of molybdenite was also evaluated.

So far, different reducing agents such as C, CO and H_2 have been used for LEMR. The reduction of ores with carbon and carbon monoxide (coal) is not environmentally friendly. These reactions produce poisonous gases such as SO_2, CO and large amount of CO_2. Hydrogen is an uncommon and expensive reducing agent in the industrial extraction of metals. In comparison, reduction of ores with methane produces less CO_2 and CO and not any SO_2. There are countries in the world where coal is not abundant but large sources of natural gas are available. Therefore using methane or natural gas for the ore reduction processes in these countries will be economically beneficial and environmentally favorable.

A good number of investigations have been reported in recent years on the lime-enhanced hydrogen, carbon and carbon monoxide reduction of molybdenite in the presence of lime. Whereas, no study has been conducted on the use of methane for such a reduction. It is the purpose of the present investigation to study the thermodynamic aspects of molybdenite reduction by methane-containing gases in the presence of lime.

---

* Corresponding author. Tel.: +98 311 391 2750; fax: +98 311 391 2752.
E-mail addresses: samad_ghasemi@yahoo.com, samadghas@ma.iut.ac.ir (S.G. Najafabadi).

0040-6031/$ – see front matter © 2010 Elsevier B.V. All rights reserved.
doi:10.1016/j.tca.2010.03.006

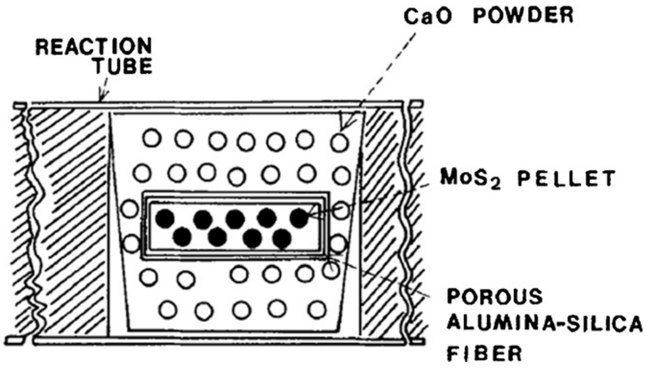

Fig. 1. Configuration of physically separated molybdenite and lime to prevent calcium molybdate formation [7].

2. Thermodynamics of the MoS_2–CH_4–CaO system

2.1. System identification

The study of thermodynamic phase equilibria provides a basic understanding of the chemical reactions prior to designing suitable reaction experiments. The best way to present thermodynamic calculation results is by stability diagrams. These diagrams provide a useful guideline for the selection of processing conditions (such as reaction temperature, pressure and reactant concentration) in which desired reaction products could be stable. The following analysis was carried out by using relevant thermodynamic sources [6]. There are six elements in the MoS_2–CaO–CH_4 system, i.e. Mo–Ca–S–O–C–H. Analysis of equilibrium state in such multi-component systems is complex. The complexity is due to the various reactions encountered among different phases present in the system. However, it shall be noticed that due to high affinity of calcium for sulfur, in the presence of excess lime (Ca/Mo > 2), all the sulfur is captured by calcium, forming calcium sulfide with a fixed activity equal to one. So, the system (Mo–Ca–S–O–C–H) can be simplified and a four component system (Mo–O–C–H) considered instead. In other words, molybdenite is thermodynamically unstable in contact with lime. When molybdenite and lime powders are intimately mixed and reacted in oxidizing atmosphere, calcium molybdate will form [7]:

$$MoS_2 + 3CaO + \tfrac{1}{2}O_2 \rightarrow CaMoO_4 + 2CaS,$$

$$\Delta G^\circ = -301476 + 36.88T (\mathrm{J\,mol^{-1}}) \qquad (1)$$

To prevent calcium molybdate formation, lime and molybdenite must be physically separated, as shown in Fig. 1 [7]. In this configuration, the reaction between molybdenite and lime in the oxidizing atmosphere proceeds as follows:

$$MoS_2 + 2CaO \rightarrow MoO_2 + 2Cas,$$

$$\Delta G^\circ = 12430 - 21.94T (\mathrm{J\,mol^{-1}}) \qquad (2)$$

According to Eqs. (1) and (2), the calcium and sulfur of the system form a neutral component, i.e. calcium sulfide. Therefore the Mo–O–C–H system (in the case of MoO_2 reduction with methane-containing gases) or the Mo–Ca–O–C–H system (in the case of $CaMoO_4$ reduction with methane-containing gases) can be studied instead of the Mo–Ca–S–O–C–H system.

2.2. Methane cracking

The main problem in reduction with methane is methane decomposition also known as methane cracking:

$$CH_4(g) = C + 2H_2(g), \quad \Delta G^\circ = 90129 - 109.4T (\mathrm{J\,mol^{-1}}) \qquad (3)$$

The affinity for carbon deposition from methane decomposition is affected by thermodynamic factors such as gas composition, temperature and total pressure of the system. Reduction at high temperatures and low pressures will promote carbon deposition according to Eq. (3). Decreasing methane partial pressure (e.g. using CH_4–H_2–Ar gas mixture instead of pure CH_4) will reduce methane cracking potential. Kinetic factors such as surface characteristics of solid species also affect carbon deposition. For example, unlike iridium and molybdenum carbide, nickel and iron catalyze methane cracking [8]. Deposition of solid carbon on the surface of reducing sample not only decreases the utilization of methane, but also hinders the further progress of the reduction by blocking the surface pores.

2.3. Thermodynamic equilibria of Mo, Mo_2C and MoC with CH_4–H_2 gas mixtures

In pyrometallurgical reduction processes, CH_4–H_2 gas mixtures can be used instead of pure CH_4 to reduce the thermodynamic potential of carbon deposition [9–11]. The effect of methane partial pressure in CH_4–H_2 gas mixture on the thermodynamics of LEMR will be investigated in this section.

As mentioned before, due to sulfur removal from molybdenite and calcium sulfide formation as a neutral phase, the Mo–O–C–H system can be considered instead of Mo–Ca–S–O–C–H. After long time flowing of reducing gas over the condensed phase, oxygen is also removed as CO_2 and/or H_2O. Thus the system will be simplified to Mo–C–H. In this system at constant pressure, according to Gibbs phase rule, the maximum number of phases in equilibrium is 4 which are 3 condensed phases and a gas phase:

$$C = 3(\mathrm{Mo, H, C}) \rightarrow F = C - P + 1 = 3 - P + 1, \quad F = 0 \rightarrow P = 4 \qquad (4)$$

this means that three condensed phases can coexist in equilibrium with a gas phase in an invariant point in the stability diagram. For such a 3-component system:

$$F = C - P + 1 = 3 - P + 1 = 4 - P \qquad (5)$$

hence, for equilibrium between gas phase and two condensed phases ($P = 3$), there is one degree of freedom that can be selected as temperature or CH_4 partial pressure in the gas mixture. In this case, the equilibrium will be represented by a line in the stability diagram. The equilibrium lines can be constructed between gas phase and each pair of condensed phases, i.e. Mo–Mo_2C, Mo_2C–MoC and MoC–C(deposited carbon). Therefore:

$$C = N - R \rightarrow R = 3 \qquad (6)$$

where, R is the number of independent reactions, C is the number of components ($C = 3$, i.e. Mo, C and H) and N is the number of species in the system ($N = 6$, i.e. Mo, Mo_2C, MoC, C(deposited carbon), CH_4(g), H_2(g)). The 3 independent chemical reactions can be written as:

$$CH_4(g) = C + 2H_2(g), \quad \mathrm{Ln}\left(\frac{P_{H_2}^2}{P_{CH_4}}\right) = \frac{-10911}{T} + 13.21 \qquad (7)$$

$$Mo_2C + CH_4(g) = 2MoC + 2H_2(g),$$

$$\mathrm{Ln}\left(\frac{P_{H_2}^2}{P_{CH_4}}\right) = \frac{-9418}{T} + 11.86 \qquad (8)$$

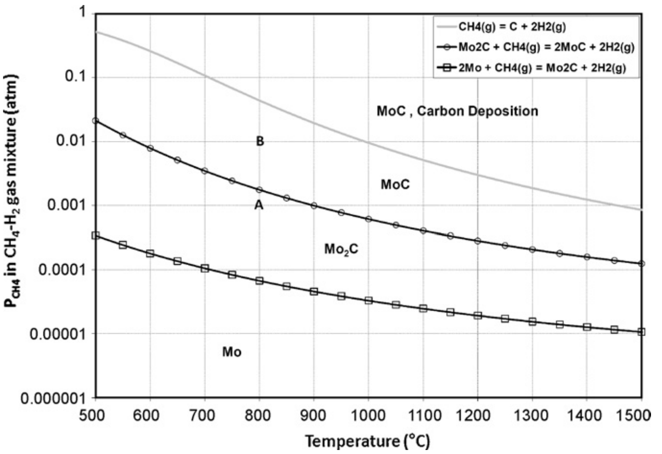

Fig. 2. Stability diagram of molybdenum and its carbides in contact with CH_4–H_2 gas mixture.

$$2Mo + CH_4(g) = Mo_2C + 2H_2(g),$$

$$\mathrm{Ln}\left(\frac{P^2_{H_2}}{P_{CH_4}}\right) = \frac{-4954}{T} + 14.21 \qquad (9)$$

assuming hydrogen and methane as the only components of the gas phase and total pressure to be one atmosphere:

$$P_t = P_{H_2} + P_{CH_4} = 1\ \text{atm} \qquad (10)$$

Eqs. (7), (10) or (8), (10) or (9), (10) can be combined and the equilibrium methane partial pressure (P_{CH_4} in CH_4–H_2 gas mixture) can be calculated for carbon deposition, Mo_2C–MoC and Mo–Mo_2C equilibria respectively at different temperatures. Fig. 2 represents the stability diagram of Mo–C–H system in methane partial pressure vs. temperature coordinates.

2.4. Thermodynamic equilibria of Mo, Mo_2C and MoC with CH_4–H_2–Ar gas mixtures

Dilution of CH_4 or CH_4–H_2 mixture with a neutral gas (e.g. Ar) will also reduce the methane cracking potential [12–17]. If the total pressure assumed to be 1 atm:

$$P_{CH_4} + P_{H_2} + P_{Ar} = 1 \Rightarrow P_{CH_4} + P_{H_2} + P_{Ar} = 1 - P_{Ar} \qquad (11)$$

where, P_{Ar} is the partial pressure of argon in CH_4–H_2–Ar gas mixture.

Combining Eqs. (7), (11) or (8), (11) or (9), (11), the equilibrium partial pressure of methane can be calculated for carbon deposition, Mo_2C–MoC and Mo–Mo_2C equilibriums respectively at different temperatures. The lines are plotted as a function of temperature at different argon partial pressures (Fig. 3).

2.5. Thermodynamic equilibria of molybdenum-containing phases with methane-oxidizing agent gas mixtures

In reduction of ores with methane, using catalytic reformed methane with H_2O and/or CO_2 (Eqs. (8) and (9)) or partially oxidized methane (Eq. (10)) is more practical than CH_4–H_2(–Ar) gas mixtures.

$$CO_2\ \text{reforming}:\ CH_4 + CO_2 = 2CO + 2H_2 \qquad (12)$$

$$H_2O\ \text{reforming}:\ CH_4 + H_2O = CO + 3H_2 \qquad (13)$$

$$\text{partial oxidation}:\ CH_4 + \tfrac{1}{2}O_2 = CO + 2H_2 \qquad (14)$$

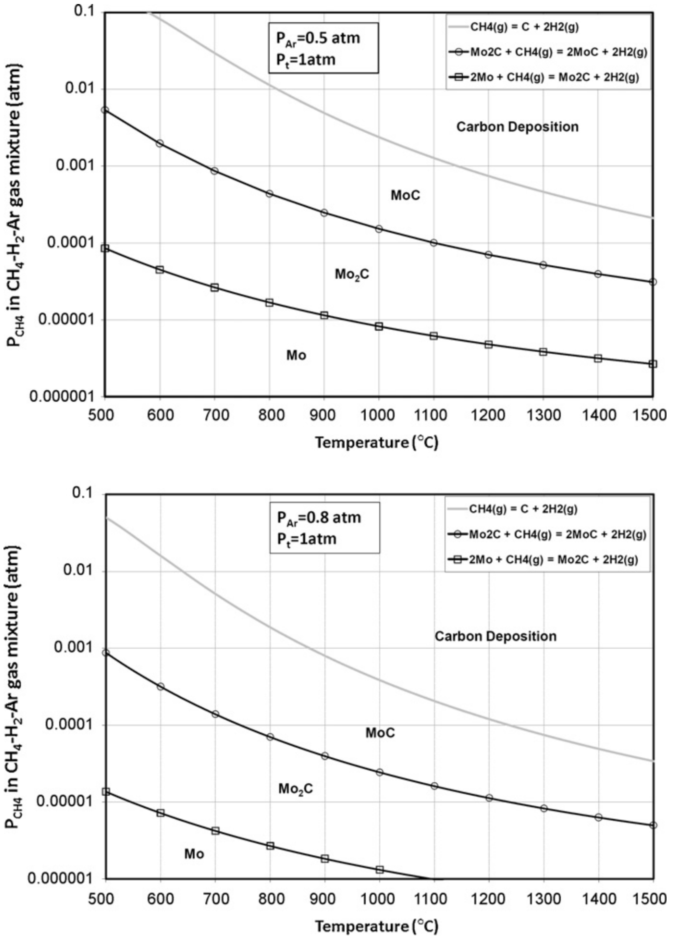

Fig. 3. Stability diagrams of molybdenum and its carbides in contact with: (a) CH_4–H_2–50% Ar gas mixture, (b) CH_4–H_2–80% Ar gas mixture.

The reformed or partially oxidized gas is a mixture of CH_4, CO, CO_2, H_2 and H_2O. The equilibrium partial pressure of each gas and thus, the reducing and carburizing power of gas mixture depends on parameters such as temperature, total pressure and CH_4/H_2O, CH_4/CO_2 and CH_4/O_2 ratios in initial gas before reforming. To define the gas chemical composition, R_C and R_H ratios can be used:

$$R_H = \frac{n_H}{n_O} = \frac{2P_{H_2} + 2P_{H_2O} + 4P_{CH_4}}{P_{H_2O} + P_{CO} + 2P_{CO_2}} \qquad (15)$$

$$R_C = \frac{n_C}{n_O} = \frac{P_{CH_4} + P_{CO} + P_{CO_2}}{P_{H_2O} + P_{CO} + 2P_{CO_2}} \qquad (16)$$

where P_i is the partial pressure of the gas *i*. The reducing power of gas will be increased if R_C and R_H are increased. Also, gases with higher R_C have higher carburizing power. If no carbon deposition occurs during reforming and if no carburizing or decarburizing reactions occur during reduction step, the R_C and R_H will not change during reforming or reducing reactions.

The reduction/carburization of MoO_2 using reformed methane gases can be presented by Mo–C–H–O system. At constant temperature and pressure, Gibbs phase rule for this system gives:

$$F = C - P = 4 - P$$

Three-phase equilibria (two solid and one gas phase) in this 4-component system (Mo–C–H–O system) at constant temperature and pressure has one degree of freedom:

$$F = C - P = 4 - 3 = 1 \qquad (17)$$

The solid–solid equilibrium line in stability diagrams has one degree of freedom (e.g. R_H). In reduction experiments, the equilibrium is among two condensed phases (e.g. Mo–Mo_2C), and gas phase containing CH_4, CO, CO_2, H_2 and H_2O components. Thus, the number of species of the system is 7. The number of independent reactions, R, in equilibrium between two solids is:

$$R = N - C = 7 - 4 = 3 \tag{18}$$

Using three independent chemical reactions and assuming constant pressure of the system to be 1 atm:

$$P_t = P_{H_2} + P_{H_2O} + P_{CO} + P_{CO_2} + P_{CH_4} = 1 \text{ atm} \tag{19}$$

and considering the activity of solids to be 1 (pure solid phases), we have a 4-equation, 5-variable nonlinear equation system. The equations are 3 independent chemical reactions and reaction 19 and the variables of the system are the partial pressure of CH_4, CO, CO_2, H_2 and H_2O. To solve the equation system, the 5th equation assumed to be Eq. (15). Solving it at any R_H, the partial pressure of gases can be obtained and partial pressures of CH_4, CO, CO_2, H_2 and H_2O will be identified. Using the following equations, the carbon, hydrogen and oxygen atomic percent in the gas can be calculated:

$$n_C = n_{CH_4} + n_{CO} + n_{CO_2} \tag{20}$$

$$n_H = 4 \times n_{CH_4} + 2 \times n_{H_2} + 2 \times n_{H_2O} \tag{21}$$

$$n_O = n_{H_2O} + n_{CO} + 2 \times n_{CO_2} \tag{22}$$

and regarding that n_i is proportional to P_i:

$$\%C = \frac{n_C}{n_C + n_H + n_O} \times 100 = \frac{P_{CH_4} + P_{CO} + P_{CO_2}}{5 \times P_{CH_4} + 2 \times P_{H_2} + 3 \times P_{H_2O} + 2 \times P_{CO} + 3 \times P_{CO_2}} \times 100 \tag{23}$$

$$\%H = \frac{n_H}{n_C + n_H + n_O} \times 100 = \frac{4 \times P_{CH_4} + 2 \times P_{H_2} + 2 \times P_{H_2O}}{5 \times P_{CH_4} + 2 \times P_{H_2} + 3 \times P_{H_2O} + 2 \times P_{CO} + 3 \times P_{CO_2}} \times 100 \tag{24}$$

$$\%O = 100 - (\%C + \%H) = \frac{P_{H_2O} + P_{CO} + 2 \times P_{CO_2}}{5 \times P_{CH_4} + 2 \times P_{H_2} + 3 \times P_{H_2O} + 2 \times P_{CO} + 3 \times P_{CO_2}} \times 100 \tag{25}$$

Thus, the equilibrium line between two solids can be plotted in C–H–O ternary diagrams at constant temperature and pressure. The equilibrium line must be constructed between each pair of the solids in Mo–C–H–O system, i.e. MoO_3-MoO_2, MoO_2–Mo, Mo–Mo_2C and MoC–Mo_2C. Also, reduction of calcium molybdate to molybdenum ($CaMoO_4$–Mo equilibrium line) and carbon deposition area must be identified in stability diagrams.

2.5.1. Equilibrium line among MoO_3-MoO_2

The independent chemical reactions for MoO_3 reduction to MoO_2 can be written as:

$$MoO_3 + CO(g) = MoO_2 + CO_2(g)$$

$$\mathrm{Ln}\left(\frac{P^2_{CO_2}}{P_{CO}}\right) = \frac{21215}{T} - 8.023 \tag{26}$$

$$MoO_3 + H_2 = MoO_2 + H_2O \quad \mathrm{Ln}\left(\frac{P_{H_2O}}{P_{H_2}}\right) = \frac{17384}{T} - 4.514 \tag{27}$$

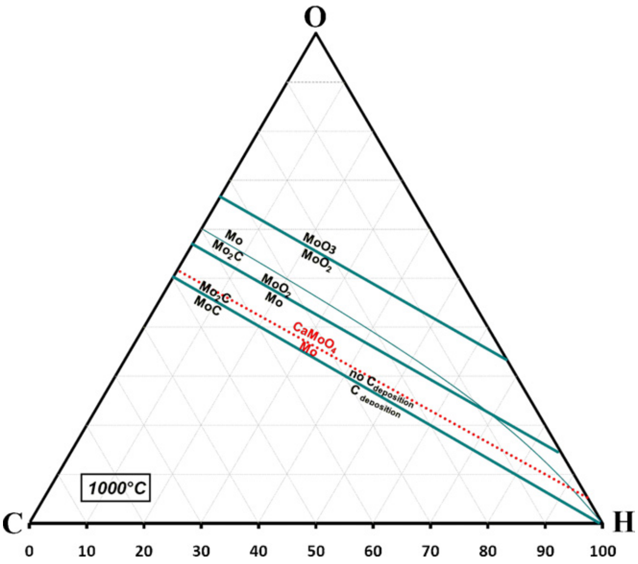

Fig. 4. Solid–solid equilibrium lines in Mo–C–H–O system at 1000 °C.

$$4MoO_3 + CH_4(g) = 4MoO_2 + CO_2(g) + 2H_2O(g)$$

$$\mathrm{Ln}\left(\frac{P^2_{H_2O}P_{CO_2}}{P_{CH_4}}\right) = \frac{46174}{T} + 8.842 \tag{28}$$

Using these equations and equation 19, the gas equilibrium partial pressures can be calculated at different R_H values. Thus the equilibrium line between MoO_2 and MoO_3 can be plotted in C–H–O ternary diagrams at any temperature. For example, the equilibrium line at 1000 °C is plotted in Fig. 4. Table 1 presents calculation results for MoO_2–MoO_3 equilibria at 700 °C.

2.5.2. Equilibrium line among MoO_2–Mo

In this equilibrium, the independent chemical reactions are:

$$\tfrac{1}{2}MoO_2 + CO(g) = \tfrac{1}{2}Mo + CO_2(g) \quad \mathrm{Ln}\left(\frac{P^2_{CO_2}}{P_{CO}}\right) = \frac{-677}{T} - 0.217 \tag{29}$$

$$\tfrac{1}{2}MoO_2 + H_2 = \tfrac{1}{2}Mo + H_2O \quad \mathrm{Ln}\left(\frac{P_{H_2O}}{P_{H_2}}\right) = \frac{-4509}{T} + 3.292 \tag{30}$$

$$2MoO_2 + CH_4(g) = 2Mo + CO_2(g) + 2H_2O(g)$$

$$\mathrm{Ln}\left(\frac{P^2_{H_2O}P_{CO_2}}{P_{CH4}}\right) = \frac{-41398}{T} + 40.07 \tag{31}$$

At different R_H values, using Eqs. (19) and (29)–(31), the system can be solved and carbon and hydrogen atomic percent in the equilibrium gas will be identified (Eqs. (20)–(25)). Thus the MoO_2 reduction to Mo equilibrium line can be constructed. For example, the equilibrium line at 1000 °C is plotted in Fig. 4.

2.5.3. Equilibrium line among Mo–Mo_2C

The independent chemical reactions for molybdenum carburization to Mo_2C can be written as:

$$2Mo + CH_4 = Mo_2C + 2H_2 \quad \mathrm{Ln}\left(\frac{P^2_{H_2}}{P_{CH_4}}\right) = \frac{-4954}{T} + 14.21 \tag{32}$$

Table 1

MoO_2–MoO_3-gas phase equilibria at 700 °C at different R_H values (at this temperature the equilibrium constants of reactions 14–16 are: $K_{14} = 6.96 \times 10^{+5}$, $K_{15} = 4.41 \times 10^{+5}$ and $K_{16} = 7.05 \times 10^{+23}$).

R_H	Equilibrium gas composition (total pressure = 1atm)					n_C	n_H	n_O	%C	%H	%O
	P_{H_2}	P_{CO_2}	P_{H_2O}	P_{CH_4}	P_{CO}						
1.984	2.3×10^{-06}	4.0×10^{-03}	1.0	5.6×10^{-27}	5.8×10^{-09}	0	2.0	1.0	0.0	66.7	33.3
1.626	2.0×10^{-06}	1.0×10^{-01}	9.0×10^{-01}	1.2×10^{-25}	1.5×10^{-07}	0.1	1.8	1.1	3.4	59.8	36.8
1.327	1.8×10^{-06}	2.0×10^{-01}	8.0×10^{-01}	1.8×10^{-25}	2.9×10^{-07}	0.2	1.6	1.2	6.7	53.2	40.1
1.074	1.6×10^{-06}	3.0×10^{-01}	7.0×10^{-01}	2.1×10^{-25}	4.3×10^{-07}	0.3	1.4	1.3	10.0	46.6	43.4
0.856	1.4×10^{-06}	4.0×10^{-01}	6.0×10^{-01}	2.0×10^{-25}	5.8×10^{-07}	0.4	1.2	1.4	13.4	40.0	46.7
0.667	1.1×10^{-06}	5.0×10^{-01}	5.0×10^{-01}	1.8×10^{-25}	7.2×10^{-07}	0.5	1.0	1.5	16.7	33.4	50.0
0.502	9.1×10^{-07}	6.0×10^{-01}	4.0×10^{-01}	1.4×10^{-25}	8.6×10^{-07}	0.6	0.8	1.6	20.0	26.7	53.3
0.356	6.9×10^{-07}	7.0×10^{-01}	3.0×10^{-01}	9.0×10^{-26}	1.0×10^{-06}	0.7	0.6	1.7	23.3	20.1	56.6
0.226	4.6×10^{-07}	8.0×10^{-01}	2.0×10^{-01}	4.7×10^{-26}	1.1×10^{-06}	0.8	0.41	1.8	26.6	13.5	59.9
0.109	2.4×10^{-07}	9.0×10^{-01}	1.0×10^{-01}	1.4×10^{-26}	1.3×10^{-06}	0.9	0.21	1.9	29.9	6.9	63.2
0.005	1.0×10^{-08}	1.0	4.6×10^{-03}	3.0×10^{-29}	1.4×10^{-06}	1.0	0	2.0	33.3	0.0	66.7

$$H_2O + CO = H_2 + CO_2 \quad \mathrm{Ln}\left(\frac{P_{H_2}P_{CO_2}}{P_{CO}P_{H_2O}}\right) = \frac{3831}{T} - 3.51 \qquad (33)$$

$$Mo_2C + CO_2 = 2Mo + 2CO \quad \mathrm{Ln}\left(\frac{P_{CO}^2}{P_{CO_2}}\right) = \frac{-26069}{T} + 19.70 \qquad (34)$$

Applying Eqs. (32)–(34) and Eq. (19), the system can be solved at different R_H and the Mo–Mo_2C equilibrium line can be constructed in C–H–O ternary diagrams. For example, the equilibrium line at 1000 °C is plotted in Fig. 4.

2.5.4. Equilibrium line among MoC–Mo_2C

The equilibrium independent chemical reactions are:

$$H_2O + CO = H_2 + CO_2 \quad \mathrm{Ln}\left(\frac{P_{H_2}P_{CO_2}}{P_{CO}P_{H_2O}}\right) = \frac{3831}{T} - 3.51 \qquad (33)$$

$$Mo_2C + CH_4 = 2MoC + 2H_2 \quad \mathrm{Ln}\left(\frac{P_{H_2}^2}{P_{CH_4}}\right) = \frac{-9418}{T} + 11.86 \qquad (35)$$

$$2MoC + CO_2 = Mo_2C + 2CO \quad \mathrm{Ln}\left(\frac{P_{CO}^2}{P_{CO_2}}\right) = \frac{-21605}{T} + 22.06 \qquad (36)$$

The system can be solved at different R_H values by using Eqs. (33), (35), (36) and (19) and thus, the atomic percent of carbon, hydrogen and oxygen will be identified using Eqs. (20)–(25). Thus the equilibrium line of Mo_2C carburization to MoC can be constructed. For example, the equilibrium line at 1000 °C is plotted in Fig. 4.

2.5.5. Equilibrium line of methane cracking (carbon deposition)

The C-H-O system must be analyzed to identify the carbon deposition area in stability diagrams. In this system, at constant temperature and pressure, according to Gibbs phase rule:

$$F = C - P = 3 - P \qquad (37)$$

To have one degree of freedom (equilibrium line between carbon deposition area and safe area in stability diagrams), we have two phases, i.e. a gas phase (CH_4–CO–CO_2–H_2–H_2O mixture) and deposited solid carbon (soot). Thus the system has 6 compounds ($N = 6$). The number of independent chemical reactions is:

$$R = N - C = 6 - 3 = 3 \qquad (38)$$

The independent reactions can be written as:

$$CH_4 = C + 2H_2 \quad \mathrm{Ln}\left(\frac{P_{H_2}^2}{P_{CH_4}}\right) = \frac{-10911}{T} + 13.21 \qquad (3)$$

$$H_2O + C = CO + H_2 \quad \mathrm{Ln}\left(\frac{P_{CO}P_{H_2}}{P_{H_2O}}\right) = \frac{-16281}{T} + 17.19 \qquad (39)$$

$$CO_2 + C = 2CO \quad \mathrm{Ln}\left(\frac{P_{CO}^2}{P_{CO_2}}\right) = \frac{-20113}{T} + 20.70 \qquad (40)$$

At any R_H value, using Eqs. (3), (39) and (40) and considering constant pressure of the system to be 1 atm (Eq. (19)), the gas composition will be identified and the related carbon, hydrogen and oxygen atomic percents can be calculated according to Eqs. (20)–(25). The carbon deposition boundary at 1000 °C is plotted in Fig. 4. This equilibrium line at 1000 °C is coincident with Mo_2C–MoC equilibrium line.

2.5.6. Equilibrium line among $CaMoO_4$–Mo

As mentioned above, when molybdenite and lime powders are intimately mixed and reacted in oxidizing atmosphere, calcium molybdate will form according to Eq. (1). Thus the equilibrium line among calcium molybdate and molybdenum must also be plotted in stability diagrams. This line identifies the minimum reducing power of gas for calcium molybdate reduction to molybdenum metal.

The reduction/carburization of $CaMoO_4$ using reformed methane gases can be presented by Mo–Ca–C–H–O system. At constant temperature and pressure, Gibbs phase rule for this system gives:

$$F = C - P = 5 - P \qquad (41)$$

Four-phase equilibria (three solid and one gas phase) in this 5-component system (Mo–Ca–C–H–O system) at constant temperature and pressure has one degree of freedom:

$$F = C - P = 5 - 4 = 1 \qquad (42)$$

The solid–solid equilibrium line in stability diagrams has one degree of freedom (e.g. R_H). In reduction experiments, the equilibrium is among three condensed phases, i.e. Mo–$CaMoO_4$–CaO, and a gas phase containing CH_4, CO, CO_2, H_2 and H_2O components. Thus, the number of species of the system is 8. The number of independent reactions, R, in equilibrium between two solids is:

$$R = N - C = 8 - 5 = 3 \qquad (43)$$

Using three independent chemical reactions:

$$\tfrac{1}{3}CaMoO_4 + H_2 = \tfrac{1}{3}Mo + H_2O + \tfrac{1}{3}CaO \quad \mathrm{Ln}\left(\frac{P_{H_2O}}{P_{H_2}}\right) = \frac{-5582}{T} + 2.23 \qquad (44)$$

$$\tfrac{1}{3}CaMoO_4 + CO = \tfrac{1}{3}Mo + CO_2 + \tfrac{1}{3}CaO \quad \mathrm{Ln}\left(\frac{P_{CO_2}}{P_{CO}}\right) = \frac{-1750}{T} - 1.24 \qquad (45)$$

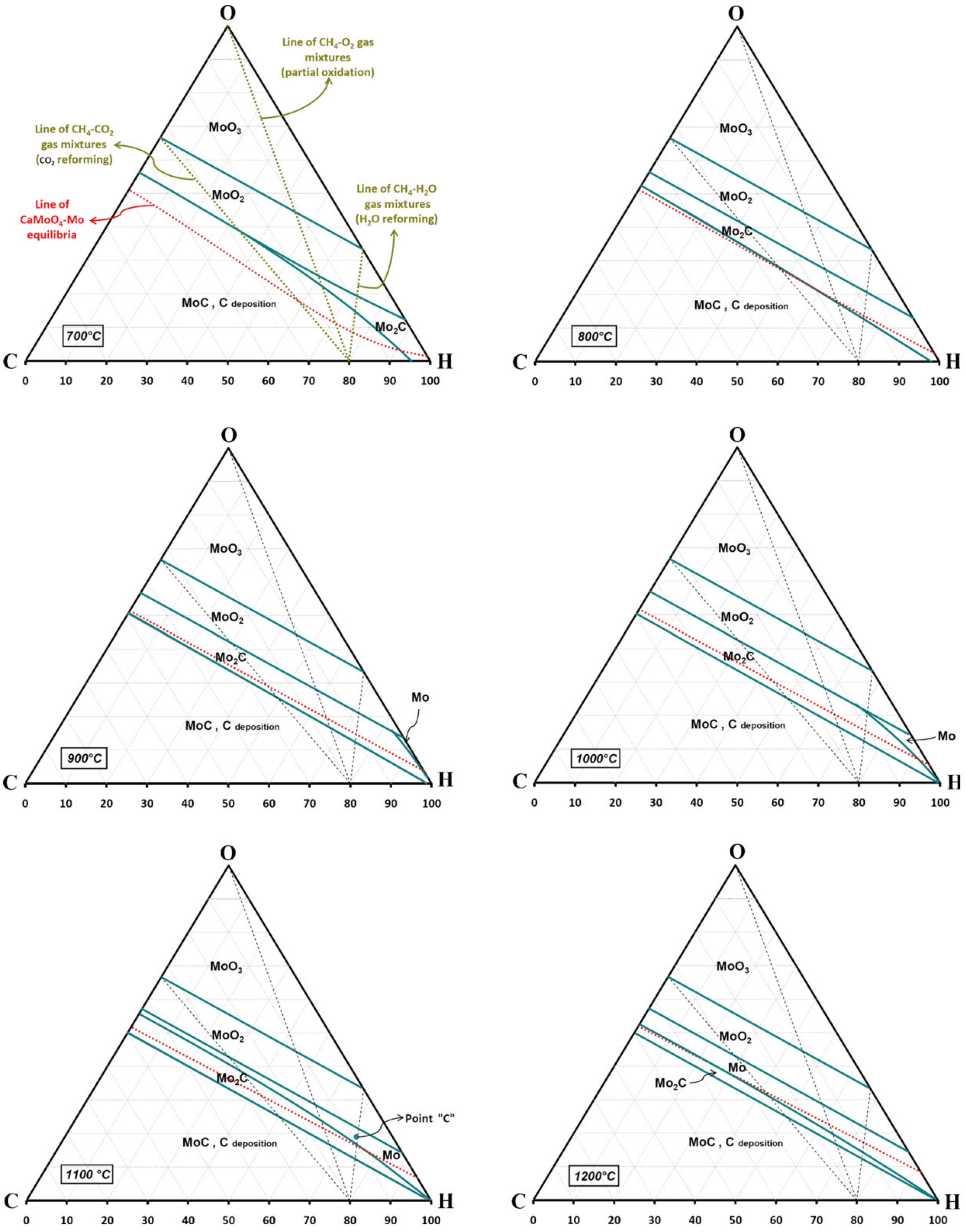

Fig. 5. Ternary stability diagram of Mo–C–H–O system at different temperatures (ternary diagrams are in atomic percent scale).

$$\tfrac{4}{3}\mathrm{CaMoO_4} + \mathrm{CH_4(g)} = \tfrac{4}{3}\mathrm{Mo} + \mathrm{CO_2(g)} + 2\mathrm{H_2O(g)} + \tfrac{4}{3}\mathrm{CaO}$$

$$\mathrm{Ln}\left(\frac{P_{\mathrm{H_2O}}^2 P_{\mathrm{CO_2}}}{P_{\mathrm{CH_4}}}\right) = \frac{-45698}{T} + 35.97 \qquad (46)$$

Using Eqs. (44)–(46) at constant pressure (Eq. (19)) and constant R_H, the equilibrium gas composition and the related %C and %H can be identified for calcium molybdate reduction to molybdenum. The dashed lines in Figs. 4–6 are $\mathrm{CaMoO_4}$–Mo equilibrium lines.

After thermodynamic calculations according to Sections 2.5.1–2.5.6, the stability diagrams of Mo–C–H–O system can be constructed at different temperatures. The stability diagrams are presented in Fig. 5 for the temperature range 700–1200 °C. The stability diagrams can also be presented by R_C vs. R_H diagrams. The diagrams have been shown in Fig. 6.

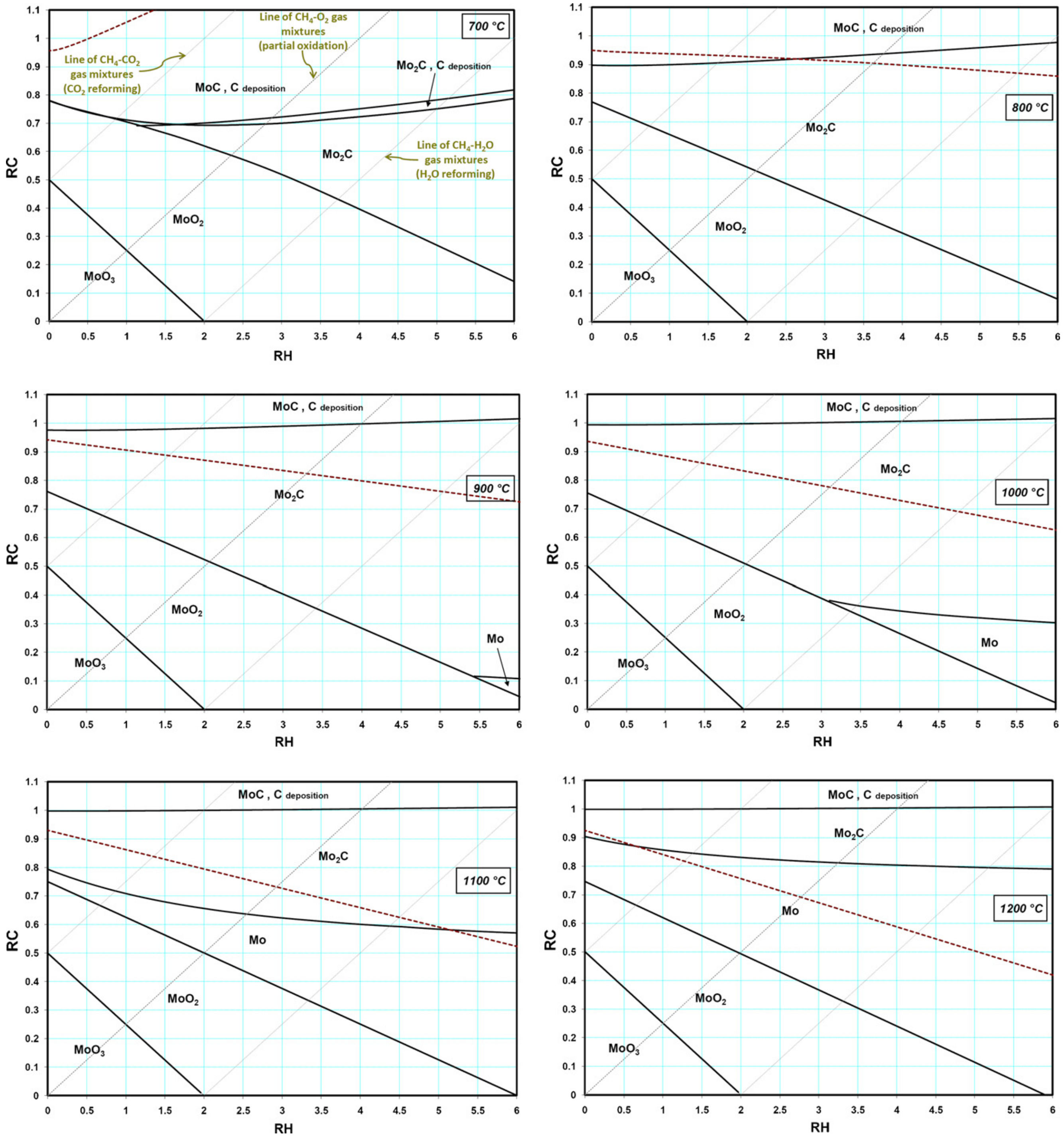

Fig. 6. R_C–R_H stability diagram of Mo–C–H–O system at different temperatures.

To attain any point in the C–H–O ternary diagrams or in the R_C–R_H stability diagrams, the suitable gas mixture must be used. For example, %C, %H and %O of the 67%CH_4–33%H_2O gas mixture respectively are 11%, 73% and 18% ($R_C = 0.5$ and $R_H = 4$). Heating the gas mixture at 1100 °C to attain thermodynamic equilibria and exposing it to MoO_3, will result in molybdenum metal stability at this temperature according to Fig. 5. This point illustrated by "C" at 1100 °C in this figure. Other points in the stability diagram can be attained in the same manner by using suitable gas mixtures. For example, CH_4–CO_2, CH_4–O_2 and CH_4–H_2O gas mixtures are presented in Figs. 5 and 6.

3. Discussion

3.1. *Effect of reducing gas composition on the reduction products*

According to the stability diagram in Fig. 2, the maximum methane partial pressure in CH_4–H_2 gas mixture at which no carbon deposition occurs can be obtained at any temperature. The stability areas of molybdenum metal and molybdenum carbides (Mo_2C and MoC) are also specified in Fig. 2. The methane instability as well as the carburization potential would be increased by increasing CH_4 partial pressure in CH_4–H_2 gas mixture. Molybdenum metal, Mo_2C and MoC will be stable phases respectively at higher carburization potential. For example, if lime and molybdenite are physically separated (Fig. 1), reduction in H_2–0.1%CH_4 atmosphere at 800 °C will result in Mo_2C formation (point A in Fig. 2) while reducing in H_2–1%CH_4 will result in MoC formation (point B in Fig. 2) without carbon deposition problem. Similar to Fig. 2, the susceptive gas compositions for carbon deposition and suitable gas for thermodynamic stability of molybdenum and its carbides can be identified in contact with CH_4–H_2–Ar gas mixtures in Fig. 3.

As can be seen in Figs. 2 and 3, the maximum methane partial pressure in reducing gas for reduction experiments without carbon deposition problem is very low (e.g. 5%CH_4–95%H_2 at 800 °C). Thus, in such methane-dilute gas mixtures, the benefits of methane would not achieve worthy. It must be notified that the stability diagrams (Figs. 2 and 3) are based on thermodynamic calculations and experimental results may be far from thermodynamic equilibrium. For example, Li et al. [18], Teixeira et al. [19] and Claridge et al. [8] reported Mo_2C formation from MoO_3 reduction with 20%CH_4–80%H_2 gas mixture in 800–1000 °C temperature range. More importantly, no carbon deposition was observed over the Mo_2C during reduction. This is where using 20%CH_4–80%H_2 reducing gas at 800 °C, MoC formation in carbon deposition area has been predicted by thermodynamic considerations (Fig. 2).

Fig. 5 represents the phase stability of molybdenum compounds in LEMR with different reformed methane gases. According to these diagrams, when molybdenite and lime are physically separated (Fig. 1), the reduction products will be MoO_3, MoO_2, Mo, Mo_2C or MoC depending on temperature and gas composition. Increasing the methane to oxidizing agent ratio (e.g. CH_4 to CO_2 ratio), the R_H and R_C will rise up and therefore the reducing and carburizing potential of gas will be increased. Increasing the reducing and carburizing potential of gas will result in the following transition steps:

$$MoO_3 \rightarrow MoO_2 \rightarrow Mo \rightarrow Mo_2 \rightarrow CMoC \qquad (47)$$

Above critical values of R_C and R_H, the soot formation will occur. Using the stability diagrams in Fig. 5, the critical values can be obtained at any temperature. As can be seen, above 800 °C the stability area of MoC is coincident with carbon deposition area. It means that the carbon activity must be at least one for carburizing of Mo_2C to MoC:

$$Mo_2C + C = 2MoC \quad \mathrm{Ln}(K) = \mathrm{Ln}\left(\frac{a^2_{MoC}}{a_{Mo_2C}a_C}\right) = \frac{1493}{T} - 1.354 \qquad (48)$$

assuming pure MoC and Mo_2C (a_{MoC} and $a_{Mo_2C} = 1$), the carbon activity is higher than one at 829 °C and more which coordinates with stability diagrams.

CO_2-reformed gases have higher carburizing potential than partially oxidized methane and H_2O-reformed gases. Thus to stabilize molybdenum metal, H_2O-reformed gases are most suitable but to stabilize molybdenum carbide, using CO_2-reformed gases is preferred. For example, at 1000 °C, molybdenum metal is stable using 26%CH_4–74%H_2O-reformed gas (%C = 71.6%, %H = 7.3% and %O = 21.1%) where, the stability area of molybdenum metal does not coincide with CO_2-reformed gases in this temperature. The connecting line between (%C = 33.3%, %H = 0.0% and %O = 66.7%, i.e. 100%CO_2) and (%C = 0.0%, %H = 66.7% and %O = 33.3%, i.e. 100%H_2O) in stability diagrams at all temperatures in Fig. 5 represents the CO_2–H_2O gas mixtures, above which the stable phase is MoO_3 at all temperatures. It means that using any trace of reducing gas, MoO_3 will e reduced to MoO_2. The C–H–O ternary diagrams can also be used for LEMR with H_2–H_2O gas mixtures (connecting line between [100%H, 0%O] and [67%H, 33%O]) and with CO–CO_2 gas mixtures (connecting line between [50%C, 50%O] and [33%C, 67%O]).

3.2. *Effect of temperature on the reduction products*

In reduction with CH_4–H_2(–Ar) gas mixtures, the instability of methane and carbon deposition potential are increased with increasing temperature (Figs. 2 and 3). This is because of the endothermic behavior of methane decomposition reaction (Eq. (3)). When the temperature rises up, the maximum allowable methane partial pressure in CH_4–H_2(–Ar) would decrease rapidly.

In reduction with reformed methane gases, at higher temperatures, the stability of molybdenum will increase and the stability of MoC, Mo_2C and MoO_2 will decrease (Fig. 5). Using CO_2 or H_2O-reformed or partially oxidized methane at temperatures below 900 °C, metallic molybdenum formation is impossible. At 1000 °C, molybdenum metal is stable when 26%CH_4–74%H_2O-reformed gas (%C = 71.6%, %H = 7.3% and %O = 21.1%) is used and at higher temperatures, molybdenum metal would be stabilized using suitable CO_2 reformed or partially oxidized methane.

3.3. *Effect of sample preparation on the reduction products*

As mentioned above, when molybdenite and lime are intimately mixed, the oxidized intermediate phase is calcium molybdate (Eq. (1)). In stability diagrams (Fig. 5), the minimum reducing power of gas has been identified for reduction of calcium molybdate. The dashed line in the stability diagrams (Fig. 5) is $CaMoO_4$–Mo equilibrium line, above which the stable phase is calcium molybdate. Below the dashed line, Mo, Mo_2C and MoC are stable phases according to Sections 2.5.2 and 2.5.4. If lime and molybdenite are intimately mixed, the MoO_3 and MoO_2 areas in the stability diagrams are removed where as physically separated molybdenite and lime (Fig. 1) cause the dashed line and calcium molybdate area to be removed. As can be seen, the stability area of molybdenum and its carbides will be limited when calcium molybdate formation is possible kinetically. For example, when molybdenite and lime were physically separated, molybdenum metal can be obtained above 900 °C, but when molybdenite and lime were intimately mixed, molybdenum metal can only be obtained above 1000 °C.

4. Conclusions

Thermodynamic calculations and plotting the stability diagrams of lime-enhanced molybdenite reduction in methane-containing atmosphere has been investigated. The suitable methane partial pressure range at any temperature for the direct Mo, Mo_2C and MoC formation from LEMR with CH_4–H_2–Ar gas mixtures are predicted. Applying these data, the Mo–C–H and Mo–C–H–Ar stability diagrams are constructed. Based on the stability diagrams of Mo–C–H and Mo–C–H–Ar systems, to prevent carbon deposition according to methane cracking, reduction must be carried out at lower temperatures and lower methane partial pressures in CH_4–H_2(–Ar) gas mixture. Using appropriate gas composition and temperature, Mo, Mo_2C and MoC can be obtained without carbon deposition. Using Mo–C–H–O stability diagrams, the appropriate gas composition can be selected to obtain different molybdenum-containing products without carbon deposition. Molybdenum metal can be obtained by reducing physically separated molybdenite and lime with H_2O-reformed CH_4 above 900 °C. Reduction with suitable CO_2-reformed methane above 1100 °C can also result in molybdenum metal formation. Mo_2C can be obtained at any temperature in the 700–1200 °C range using CO_2-reformed, H_2O-reformed or partially oxidized methane without carbon deposition problem.

References

[1] C.K. Gupta, Extractive Metallurgy of Molybdenum, CRC Press, USA, 1992.

[2] T.R. Mankhand, P.M. Prasad, Metall. Mater. Trans. B 13 (1982) 275–282.
[3] P.M. Prasad, T.R. Mankhand, P.S. Rao, Miner. Eng. 6 (1993) 857–871.
[4] R. Padilla, M.C. Ruiz, H.Y. Sohn, Metall. Mater. Trans. B 28 (1997) 265–274.
[5] P.M. Prasad, P.S. Rao, S.N. Singh, A.J.K. Prasad, T.R. Mankhand, Metall. Mater. Trans. B 33 (2002) 345–354.
[6] O. Kubaschewski, C.B. Alcock, Metallurgical Thermochemistry, Pergamon Press, Oxford, 1979.
[7] H.Y. Sohn, D. Kim, Metall. Mater. Trans. B 19 (1988) 973–975.
[8] B. Claridge, P.E. York, J. Brungs, C. Marquez-Alvarez, J. Sloan, S.C. Tsang, L.H. Green, J. Catal. 180 (1998) 85–100.
[9] D. Ghosh, A.K. Roy, A. Ghosh, ISIJ 26 (1986) 187–193.
[10] G. Zhang, O. Ostrovski, Metall. Mater. Trans. B 32 (2001) 465–473.
[11] G. Zhang, O. Ostrovski, Metall. Mater. Trans. B 31 (2000) 129–139.
[12] N. Anacleto, O. Ostaovski, Metall. Mater. Trans. B 35 (2004) 609–615.
[13] O. Ostrovski, G. Zhang, AIChE J. 52 (2006) 300–310.
[14] N. Anacleto, O. Ostrovski, S. Ganguly, ISIJ 44 (2004) 1480–1487.
[15] B. Khoshandam, R.V. Kumar, E. Jamshidi, Metall. Mater. Trans. B 35 (2004) 825–828.
[16] H. Ale Ebrahim, E. Jamshidi, Ind. Eng. Chem. Res. 44 (2005) 495–504.
[17] H. Ale Ebrahim, E. Jamshidi, Ind. Eng. Chem. Res. 41 (2002) 2630–2636.
[18] S. Li, W.B. Kim, J.S. Lee, Chem. Mater. 10 (1998) 1853–1862.
[19] V.L.S. Teixeira da Silva, E.I. Ko, M. Schmal, S.T. Oyama, Chem. Mater. 7 (1995) 179–184.